

Manuscript Number:

Title: Radiomic features of cervical cancer on T2- and diffusion-weighted MRI: prognostic value in low-volume tumors suitable for trachelectomy

Article Type: Review Article

Keywords: Radiomics; MRI; cervical cancer; recurrence; trachelectomy

Corresponding Author: Professor Nandita M deSouza,

Corresponding Author's Institution: CRUK Cancer Imaging Centre, The Institute of Cancer Research and The Royal Marsden Hospital NHS Foundation Trust

First Author: Nandita M deSouza

Order of Authors: Nandita M deSouza; Thomas Ind; James Petts; James D'Arcy; Simon J Doran; Benjamin W Wormald

Abstract: Background: Textural features extracted from MRI potentially provide prognostic information additional to volume for influencing surgical management of cervical cancer.

Purpose: To identify textural features that differ between cervical tumors above and below the volume threshold of eligibility for trachelectomy and determine their value in predicting recurrence in patients with low-volume tumors.

Methods: Of 378 patients with Stage1-2 cervical cancer imaged prospectively (3T, endovaginal coil), 125 had well-defined, histologically-confirmed squamous or adenocarcinomas with >100 voxels (>0.07cm³) suitable for radiomic analysis. Regions-of-interest outlined the whole tumor on T2-W images and apparent diffusion coefficient (ADC) maps. Textural features based on gray-level co-occurrence matrices were compared (Mann-Whitney test with Bonferroni correction) between tumors greater (n=46) or less (n=79) than 4.19cm³. Clustering eliminated correlated variables. Significantly different features were used to predict recurrence (regression modelling) in surgically-treated patients with low-volume tumors and compared with a model using clinico-pathological features.

Results: Textural features (Dissimilarity, Energy, ClusterProminence, ClusterShade, InverseVariance, Autocorrelation) in 6 of 10 clusters from T2-W and ADC data differed between high-volume (mean±SD 15.3±11.7cm³) and low-volume (mean±SD 1.3±1.2cm³) tumors. (p<0.02). In low-volume tumors, predicting recurrence was indicated by: Dissimilarity, Energy (ADC-radiomics, AUC=0.864); Dissimilarity, ClusterProminence, InverseVariance (T2-W-radiomics, AUC=0.808); Volume, Depth of Invasion, LymphoVascular Space Invasion (clinico-pathological features, AUC=0.794). Combining ADC-radiomic (but not T2-radiomic) and clinico-pathological features improved prediction of recurrence compared to the clinico-pathological model (AUC=0.916, p=0.006). Findings were supported by bootstrap re-sampling (n=1000).

Conclusion: Textural features from ADC maps and T2-W images differ between high- and low-volume tumors and potentially predict recurrence in low-volume tumors.

Suggested Reviewers: Evis Sala MD, PhD, FRCR
es220@cam.ac.uk
Gynae radiology specialist

Laure Fournier MD, PhD
laure.fournier@parisdescartes.fr
Gynae radiology specialist



Pr. B Karlan
Editor in Chief,
Gynecologic Oncology

23 August 2019

Dear Professor Karlan,

Please find enclosed our manuscript entitled **“Radiomic features of cervical cancer on T2- and diffusion-weighted MRI: prognostic value in low-volume tumors suitable for trachelectomy”** for consideration for publication in Gynecologic Oncology.

Radiomic analyses, particularly in Magnetic Resonance Imaging are a burgeoning field of interest, and we feel we have brought a novel way of addressing feature selection by interrogating features that differ between high and low volume cervical tumors. Tumor volume is an established poor prognostic factor in this disease. We therefore sought to establish whether radiomic differences between high- and low-volume cervical cancers existed, and if so, whether the low-volume tumors that radiomically appeared like high-volume ones had a worse prognosis. We found that we could identify low-volume tumors at risk of recurrence using this method.

Cervical cancer is relatively rare now in countries with effective screening programmes, and tumors are often low-volume when detected. We feel this technique offers a means of flagging patients with low-volume tumors at risk of recurrence. This should enable a programme of more frequent monitoring in these often young women with potentially good life expectancy.

This was a prospective study done with IRB approval, and with written informed consent from all patients.

All authors contributed to this manuscript in one or more of the following ways: literature search, study planning, data acquisition, data analysis and manuscript drafting. In addition, all were involved in manuscript editing and final approval.

We are hopeful that you and your readers will find this work of major interest,

With kind regards,

The Institute of
Cancer Research

Professor Nandita deSouza
MD, FRCP, FRCR
Professor of Translational Imaging &
Co-Director
Cancer Research UK
Cancer Imaging Centre

Downs Road, Sutton
Surrey, SM2 5PT
T +44 20 8661 3289/3119
E nandita.desouza@icr.ac.uk
W icr.ac.uk

Registered office
The Institute of Cancer Research:
Royal Cancer Hospital
123 Old Brompton Road
London SW7 3RP

A Charity. Not for Profit.
Company Limited by Guarantee.
Registered in England No. 534147.
VAT Registration No. 849 0581 02

2 of 2



Nandita deSouza
Professor of Translational Imaging
The Institute of Cancer Research

bw_coi_disclosure

[Click here to download 2. Conflict of Interest Forms: bw_coi_disclosure.pdf](#)

jd_coi_disclosure

[Click here to download 2. Conflict of Interest Forms: jd_coi_disclosure.pdf](#)

jp_coi_disclosure

[Click here to download 2. Conflict of Interest Forms: jp_coi_disclosure.pdf](#)

nds_coi_disclosure

[Click here to download 2. Conflict of Interest Forms: nds_coi_disclosure.pdf](#)

sd_coi_disclosure

[Click here to download 2. Conflict of Interest Forms: sd_coi_disclosure.pdf](#)

ti_coi_disclosure

[Click here to download 2. Conflict of Interest Forms: ti_coi_disclosure.pdf](#)

1 **Radiomic features of cervical cancer on T2- and diffusion-weighted MRI:**
2 **prognostic value in low-volume tumors suitable for trachelectomy**

3
4 Benjamin W Wormald^a MBBS, BSc

5 Simon J Doran^a BA, PhD

6 Thomas EJ Ind^{b,c} MBBS, MD

7 James D’Arcy^a MSci, PhD

8 James Petts^a BSc, PhD

9 Nandita M deSouza^a MD, FRCR

10 ^aMRI Unit, Division of Radiotherapy and Imaging, The Institute of Cancer Research
11 and The Royal Marsden NHS Foundation Trust, Sutton, UK

12 ^bDepartment of Gynaecological Oncology, The Royal Marsden NHS Foundation
13 Trust, London, UK

14 ^cSt George’s University of London, Tooting, London, UK

15

16 **Correspondence to:**

17 Nandita deSouza

18 Professor in Translational Imaging

19 The Institute of Cancer Research

20 Downs Road

21 Sutton

22 Surrey

23 SM2 5PT

24 E: nandita.desouza@icr.ac.uk

25

26 **Running title:** *MRI Radiomics in low-volume cervical cancer*

27

28 **Keywords:** Radiomics, MRI, cervical cancer, recurrence, trachelectomy

29

30 **Financial support:** We gratefully acknowledge CRUK support to the Cancer
31 Imaging Centre at ICR and RMH in association with MRC and Department of Health
32 C1060/A10334, C1060/A16464 and NHS funding to the NIHR Biomedical Research
33 Centre and the Clinical Research Facility in Imaging.

34 BW is funded by the CRUK Imaging Centre award C1060/A16464. SD and JD are
35 funded by the CRUK National Translational Imaging Accelerator (NCITA,
36 C7273/A28677) award.

37

38 **Acknowledgements:**

39 The authors thank all the individuals who participated in this study.

40 We are grateful to Dr M Orton for his statistical advice, and to V Morgan. A
41 MacDonald and M Usher for their expert assistance with endovaginal MRI scanning.

42

43 **Conflict of interest/disclosure statement:**

44 All authors declare no potential conflicts of interest.

45 Abstract word count: **250**

46 Manuscript word count: **3707**

47 Number of Figures: **2**

48 Number of Tables: **4**

49 **Supplementary data: 2 Figures and 1 Table**

50

51 **Abbreviations**

52 ADC – Apparent diffusion co-efficient

53 ROI – Region of interest

54 AUC – Area under curve

55 DW – Diffusion weighted

56 GLCM – Grey Level co-occurrence matrix

57 ROC – Receiver operating curve

58 LLETZ – Large loop excision of transformation zone

59 LVSI – Lymphovascular space invasion

60 SNR – Signal to noise ratio

61

62

63

64 **Abstract**

65 **Background:** Textural features extracted from MRI potentially provide prognostic
66 information additional to volume for influencing surgical management of cervical
67 cancer.

68 **Purpose:** To identify textural features that differ between cervical tumors above and
69 below the volume threshold of eligibility for trachelectomy and determine their value
70 in predicting recurrence in patients with low-volume tumors.

71 **Methods:** Of 378 patients with Stage1-2 cervical cancer imaged prospectively (3T,
72 endovaginal coil), 125 had well-defined, histologically-confirmed squamous or
73 adenocarcinomas with >100 voxels ($>0.07\text{cm}^3$) suitable for radiomic analysis.
74 Regions-of-interest outlined the whole tumor on T2-W images and apparent diffusion
75 coefficient (ADC) maps. Textural features based on gray-level co-occurrence
76 matrices were compared (Mann-Whitney test with Bonferroni correction) between
77 tumors greater ($n=46$) or less ($n=79$) than 4.19cm^3 . Clustering eliminated correlated
78 variables. Significantly different features were used to predict recurrence (regression
79 modelling) in surgically-treated patients with low-volume tumors and compared with
80 a model using clinico-pathological features.

81 **Results:** Textural features (Dissimilarity, Energy, ClusterProminence, ClusterShade,
82 InverseVariance, Autocorrelation) in 6 of 10 clusters from T2-W and ADC data
83 differed between high-volume (mean \pm SD $15.3\pm 11.7\text{cm}^3$) and low-volume (mean \pm SD
84 $1.3\pm 1.2\text{cm}^3$) tumors. ($p<0.02$). In low-volume tumors, predicting recurrence was
85 indicated by: Dissimilarity, Energy (ADC-radiomics, AUC=0.864); Dissimilarity,
86 ClusterProminence, InverseVariance (T2-W-radiomics, AUC=0.808); Volume, Depth
87 of Invasion, LymphoVascular Space Invasion (clinico-pathological features,

88 AUC=0.794). Combining ADC-radiomic (but not T2-radiomic) and clinico-pathological
89 features improved prediction of recurrence compared to the clinico-pathological
90 model (AUC=0.916, $p=0.006$). Findings were supported by bootstrap re-sampling
91 (n=1000).

92 **Conclusion:** Textural features from ADC maps and T2-W images differ between
93 high- and low-volume tumors and potentially predict recurrence in low-volume
94 tumors.

95

96

97

98 **Introduction**

99 Stage 1 cervical cancer is primarily treated with hysterectomy, although less radical
100 surgical options (cone biopsy, trachelectomy) are considered where fertility
101 preservation is desirable [1-4]. Decisions regarding the type and extent of surgery
102 and the subsequent need for adjuvant therapy depend on tumor resectability and the
103 risk of recurrence. Biomarkers that predict recurrence, therefore, are of paramount
104 importance for selecting the most appropriate treatment options. In tumors >2cm in
105 longest dimension, pre-operative tumor volume is a powerful adverse prognostic
106 factor associated with reduced overall survival [5; 6]. Other prognostic factors, such
107 as tumor type, grade, lymphovascular space invasion (LVSI) and depth of stromal
108 invasion are derived from a biopsy [7-10], and therefore may not represent the tumor
109 in its entirety. Prognostic biomarkers derived from imaging would be more
110 representative of the whole tumor and would enable selection of the optimal surgical
111 management at the outset in Stage 1 disease.

112 Magnetic Resonance imaging is routinely used to detect and stage cervical cancer,
113 where T2-W and diffusion-weighted (DW) imaging form the mainstay of diagnostic
114 sequences [11; 12]. Derivation of an apparent diffusion coefficient (ADC) from the
115 DW images [13] and analysis of first order histogram distribution of ADC values has
116 been shown to predict histological subtype [14; 15], staging [16], parametrial
117 invasion [17], LVSI [18] the response to chemo-radiotherapy [19] and to aid surgical
118 decision-making [20]. However, these first-order statistical quantitative imaging data
119 remain limited in their prediction of likely recurrence [21]. It is possible to refine
120 image analysis and convert the T2-W [22] and DW [23] imaging data into a high-
121 dimensional feature space using algorithms to extract a more extensive set of
122 statistical features within the data. This type of analysis, referred to as “radiomics”,

123 requires that the data have a high signal-to-noise ratio to reduce error in the analysis
124 from image noise; this is achievable in cervical cancer using an endovaginal MRI
125 technique [24]. The purpose of this study was to identify radiomic features of cervical
126 cancers on endovaginal MRI that differed between tumors below and above the
127 volume threshold of eligibility for trachelectomy (less or greater than 4.19 cm^3 ,
128 equivalent to a 2cm diameter spherical tumor volume) and to determine their value in
129 predicting recurrence in patients in the low-volume tumor group.

130

131

132 **Methods**

133 Study Design

134 This single-institution, prospective, pilot cohort study included patients with
135 histologically confirmed cervical cancer, presumed Stage 1 or 2 (FIGO 2009 [25],
136 referred for endovaginal MRI between March 2011 and October 2018 and potentially
137 suitable for surgical management (trachelectomy or hysterectomy). This was part of
138 an on-going institutional review board (IRB) approved research study documenting
139 imaging features of cervical cancer indicative of poor outcome (NCT01937533). All
140 patients gave their written consent for use of their data. All patients were treated
141 with curative intent with either surgery or chemoradiation following MRI and staging
142 investigations. Surgical options included cold-knife cone, trachelectomy or
143 hysterectomy depending on their suitability for fertility preservation and their desire
144 for continued fertility. A pelvic lymphadenectomy was performed in all cases.

145 Clinico-pathological metrics recorded in each case were tumor volume, type, grade,
146 LVSI, parametrial invasion, Depth of Invasion and lymph node metastasis. Patients
147 were followed up for median of 35 months (3-92). Median time to recurrence was 7
148 months (3-62 months).

149

150 Study participant selection

151 378 consecutive patients were imaged over the defined study period. In 98 cases,
152 tumor was not identified on MRI while in 127 cases tumor was poorly identified and
153 volume was $<0.07 \text{ cm}^3$, (62 of these had negative histology). Of the remaining 153
154 patients, 10 had non-cervical origin tumours on histology, 12 had histology other

155 than squamous or adenocarcinoma (clear cell or neuroendocrine histology), 2 had
156 metastatic disease, in 3 the whole tumor was not within the imaged field-of-view, and
157 1 did not have a diffusion-weighted images (Supplementary data, **Figure S1**). These
158 28 exclusions resulted in 125 patients with histologically confirmed residual
159 squamous-or adeno carcinomas that could be defined on MRI and were therefore
160 eligible for analysis. No patients had to be excluded on the grounds of image artefact
161 degrading the data. In patients who underwent primary surgery, the post-operative
162 histological diagnosis was taken as the gold-standard. In those who received
163 chemoradiation therapy, their pre-treatment histological diagnosis was taken as the
164 gold-standard. In assessing lymph node status, surgical pathology was the
165 reference gold-standard in those undergoing surgery, and imaging (MRI or PET-CT)
166 was the reference gold-standard in those treated with chemoradiation.

167

168 MRI protocol

169 All scans were performed on a 3.0 Tesla Philips Achieva (Best, The Netherlands)
170 with a dedicated in-house developed 37 mm ring-design solenoidal receiver coil that
171 has been previously described (20, 21, 24). Cervical position was determined at
172 vaginal examination, after which the coil was inserted and placed around the cervix.
173 Image distortion from susceptibility artefacts were reduced by aspiration of vaginal
174 air via a 4 mm diameter tube (Ryles; Pennine Healthcare, London, England). The
175 administration of Hyoscine butyl bromide (Buscopan) 20 mg IM decreased artefacts
176 from bowel peristalsis.

177 T2-W images were obtained in three planes orthogonal to the cervix: TR/TE 2750/80
178 ms (coronal and axial) and 2500/80 ms (sagittal); field of view (FOV) 100 mm x 100

179 mm; acquired voxel size 0.42 x 0.42 x 2 mm; reconstructed voxel size 0.35 x 0.35 x
180 2 mm; slice thickness 2 mm; slice gap 0.1 mm; 24 coronal and 22 sagittal slices;
181 number of signal averages (NSA) 2. Additionally, matched Zonal Oblique Multislice
182 (ZOOM) diffusion-weighted images (DWI) were acquired: TR/TE 6500/54 ms; b-
183 values 0, 100, 300, 500, 800 s/mm²; FOV 100 x 100 mm; acquired voxel size 1.25 x
184 1.25 x 2 mm; reconstructed voxel size 0.45 x 0.45 x 2 mm; slice thickness 2 mm,
185 slice gap 0.1 mm; 24 slices, NSA 1. ADC maps were automatically generated by the
186 scanner software. These were compared with T2-W images to identify the presence
187 and extent of a tumor within the cervix. Mass-lesions disrupting the normal cervical
188 epithelial architecture that were intermediate signal-intensity on T2-W images with
189 corresponding restriction on the ADC maps were recognized as tumor.

190

191 *MRI analysis: extraction of texture features*

192 Scans were anonymised (DicomBrowser, Neuroinformatics Research Group,
193 Washington University, St Louis, MO) and transferred to an XNAT[26; 27] image
194 repository. Images were imported into OsiriX (Pixmeo SARL, Bernex, Switzerland)
195 and 2D regions-of-interest (ROI) were drawn by a radiologist, (25 years' experience)
196 on the coronal T2-W and ADC maps on every slice demonstrating tumor (**Figure 1**).
197 2D ROI contours were aggregated using a custom Python script, integrated into
198 OsiriX via pyOsirix [28] and exported as a single 3D volume (VOI) in DICOM RT-
199 STRUCT format, which was then uploaded to XNAT. Custom in-house software
200 (MATLAB, MathWorks, Natick, MA) was used to extract Grey Level Co-occurrence
201 Matrix (GLCM) features (Haralick texture analysis [29; 30]) from the both the T2-W
202 images and ADC maps.

203 Statistical analysis

204 Statistical analysis was performed with *R* (R Core Team (2019), Vienna, Austria.
205 <http://www.R-project.org>). Correlations between features indicated 10 distinct feature
206 clusters by creating a dissimilarity measure from a distance matrix (Supplementary
207 data, **Figure S2**). Several of the texture features were very highly correlated ($r=0.97-$
208 1) and were successfully clustered. The feature with the greatest dynamic range
209 from each cluster was selected for investigation (**Table S1**): these were Dissimilarity,
210 Contrast, Energy, Entropy, ClusterProminence, ClusterShade, InverseVariance,
211 Correlation, Autocorrelation and InformationalMeasureCorrelation2. Contrast and
212 Entropy, although not clustered with Dissimilarity and Energy respectively, were
213 highly correlated ($R>0.9$), and were removed.

214 A Shapiro-Wilk test revealed that features did not have a normal distribution so non-
215 parametric tests were employed. A Mann-Whitney (*U*) test with Bonferroni correction
216 was applied to assess the differences in texture features between tumors greater
217 than or less than 4.19 cm^3 on T2-W imaging (volume threshold of eligibility for
218 trachelectomy, designated as high-volume and low-volume tumors). A p-value <0.05
219 was taken to be significant. Stepwise logistic regression was used to determine
220 which combination of features from each category (ADC-radiomics, T2-W-radiomics
221 and clinico-pathological metrics) were indicative of recurrence. This was done in 2
222 scenarios i) in all patients with low-volume tumors using adjuvant therapy as a
223 feature in the model; ii) in only those patients who did not receive adjuvant therapy.
224 The logistic regression coefficients were used to combine the features identified from
225 each scenario to generate Receiver operating characteristic (ROC) curves for ADC-
226 radiomic features and for T2-W radiomic features predicting recurrence in low-
227 volume tumors. These were compared with the ROC curve of the clinico-pathological

228 features identified in both scenarios using the Akaike information criteria (AIC).
229 Further improvements in predicting recurrence were investigated by combining the
230 features identified in the ADC-radiomic and T2-W radiomic models with the clinico-
231 pathological features and evaluated with a Chi-square test. A bootstrap resampling
232 (n=1000) procedure was performed to obtain estimates of optimism in the regression
233 models to provide a bias-corrected AUC value through a Somers' D rank correlation
234 metric whereby $AUC = (1 + \text{Somers } D)/2$. The rms: Regression Modelling Strategies
235 R package, version 5.1-0 was used.

236

237

238 **Results**

239 *Patient demographics and clinical characteristics*

240 Eligible patients were aged between 24-89 years (mean 38.4 years) at primary
241 treatment. Initial diagnosis was made with biopsy in 77 patients and large loop
242 excision of the transformation zone (LLETZ) in 48 patients. Biopsies confirming the
243 presence of cancer were not large or deep enough to confirm tumor grade in 1 case
244 or LVSI in 7.

245 Of 125 patients, 79 were low-volume (range 0.26 – 4.17 cm³, mean 1.3 ± 1.2 cm³);
246 70 were treated surgically and 9 with chemoradiation. Forty-six were high-volume
247 (range 4.2-56.1 cm³, mean 15.3 ± 11.7 cm³); 7 were treated surgically and 39 with
248 chemoradiation. Of the 70 patients with low-volume tumors treated surgically, 2
249 patients did not have follow-up data, so that prediction of recurrence was modelled
250 on 68 patients (**Figure S1**). Patient and tumor characteristics in those with high- and
251 low-volume tumors are detailed in **Table 1**.

252 Fifty-four of 68 patients in the low-volume group did not receive adjuvant therapy.
253 Fourteen patients in the low-volume group received adjuvant therapy following
254 surgery because of adverse features: 5 had unexpected lymph node metastases, 3
255 had unexpected extension of tumor to the parametrium, 1 had a 0.5 mm margin to
256 the parametrium at surgical histology, 1 had spread to the vaginal cuff and 4 met 2 of
257 the Sedlis criteria (LVSI) and deep stromal invasion). There were 7 recurrences
258 overall: 5 in 54 patients who had not and 2 in 14 in patients who had received
259 adjuvant therapy.

260

261 Differences in texture features based on tumor volume and clinico-pathological
262 metrics

263 Number of voxels in the T2-W images ranged from 17441-209892 in the high-volume
264 tumors (median 38597) to 107-17324 in the low-volume tumors (median 2750).

265 Number of voxels in the ADC maps ranged from 10497-140650 in the high-volume
266 tumors (median 26812) to 75-13294 in the low-volume tumors (median 1927).

267 From heat-maps of correlated texture features (Supplementary data, **Figure S2**), ten
268 texture feature clusters were identified (Supplementary data, **Table S1**). After
269 Bonferroni correction, 6 texture features on both ADC maps and T2-W images
270 (**Table 2**) remained significantly different between the high- and low-volume tumors,
271 namely Dissimilarity, Energy, ClusterProminence, InverseVariance and
272 Autocorrelation. An additional feature on T2-W imaging (Correlation) differed
273 between groups (**Table 3**).

274 In low-volume tumors, Dissimilarity and Energy differed in patients without and with
275 LVSI. (Supplementary data, **Table S2**). However, none of the Haralick features from
276 ADC maps or T2-W images differed between adeno- and squamous cancers, low
277 and high-grade tumors, or those with negative vs. positive lymph node status.

278

279 Clinico-pathological features as predictors of recurrence

280 AUCs and 95% CI for individual clinico-pathological features for predicting
281 recurrence in all low-volume tumors (n=68) regardless of adjuvant therapy were:
282 (tumor type (0.548 [0.340-0.756]), grade (0.501 [0.294-0.709]), LVSI (0.537 [0.347-
283 0.728]) , Depth of Invasion (0.553 [0.291-0.814]), lymph node metastasis (0.530

284 [0.386-0.675]) and T2-W tumor volume (0.691 [0.448-0.934]). Adjuvant treatment
285 had an AUC of 0.544 [0.357-0.732]. When patients receiving adjuvant therapy were
286 excluded (n=54), the AUCs were: tumor type (0.555 [0.305-0.805]), grade (0.504
287 [0.254-0.754]), LVSI (0.633 [0.570-0.695]), Depth of Invasion (0.510 [0.214-0.807]),
288 lymph node metastasis (0.510 [0.490-0.530]) and T2-W tumor volume (0.629 [0.327-
289 0.931]). Regression modelling which included adjuvant therapy as a confounding
290 feature indicated that volume and Depth of Invasion were indicative of recurrence
291 (AUC=0.766 CI 0.562-0.970), but that when patients who received adjuvant therapy
292 were excluded, LVSI alone was predictive of recurrence (AUC= 0.633 95% CI 0.570-
293 0.695).

294 Combining T2-W volume, Depth of Invasion and LVSI predicted recurrence in all 68
295 low-volume tumors with an AUC 0.794 (95% CI 0.617- 0.971) and AIC of 45.684.

296

297 Texture features from ADC maps as predictors of recurrence

298 When considering all 68 patients with low-volume disease, the texture features
299 Dissimilarity, Energy, InverseVariance, ClusterProminence, ClusterShade,
300 Autocorrelation and volume derived from ADC maps had an AUC of 0.775, 0.635,
301 0.674, 0.646, 0.508, 0.665 and 0.672, respectively for predicting recurrence. (**Figure**
302 **2, Table 3**). A regression model indicated that when combined, Dissimilarity and
303 Energy were contributory to prediction of recurrence (AUC=0.864, 95% CI =0.772-
304 0.956, AIC 41.044). However, when patients who had adjuvant therapy were
305 excluded, only Dissimilarity was predictive of recurrence (AUC=0.853, 95%
306 CI=0.725-0.981).

307 Combining metrics predictive of recurrence from ADC-radiomic and clinico-
308 pathological models (Dissimilarity and Energy with T2-W volume+Depth of
309 Invasion+LVSI) significantly improved prediction of recurrence in all 68 low-volume
310 tumors (AUC=0.916, 95% CI 0.837-0.994, with 100% sensitivity, 77% specificity,
311 $p=0.006$, AIC=39.638, **Table 4**) compared to the combined clinico-pathological
312 model of T2-W volume+Depth of Invasion+LVSI.

313 Examples of tumors with high Dissimilarity, and low Energy vs. low Dissimilarity and
314 high Energy respectively are illustrated in **Figure 1**.

315

316 Texture features from T2-W imaging as prognostic biomarkers

317 When considering patients with low-volume disease, the texture features
318 Dissimilarity, Energy, InverseVariance, ClusterProminence, ClusterShade,
319 Autocorrelation, Correlation and Volume derived from T2-W images individually had
320 an area under the curve (AUC) of 0.609, 0.604,0.671, 0.607, 0.628, 0.536, 0.511 and
321 0.691 respectively for predicting recurrence (**Table 4**). When all low-volume tumors
322 were considered, a regression model indicated that no combination of features
323 improved prediction of recurrence. When patients who had adjuvant therapy were
324 excluded, Dissimilarity, Clusterprominence and InverseVariance together were
325 predictive of recurrence (AUC=0.837, 95% CI=0.698-0.976). These features applied
326 to all 68 patients gave an AUC of 0.808 (95% CI=0.690-0.926, AIC=49.193).

327 Combining metrics predictive of recurrence from T2-W-radiomic and clinico-
328 pathological models (Dissimilarity, ClusterProminence and InverseVariance with
329 LVSI+Depth of Invasion+T2-W volume) did not significantly improve prediction of

330 recurrence in low-volume tumors (AUC=0.906, 95% CI 0.822-0.991, p= 0.09,
331 AIC=45.128, **Table 4**) compared to the combined clinico-pathological model of T2-W
332 volume+Depth of Invasion+LVSI.

333

334 *Validation of logistic regression models*

335 Bias-corrected AUCs generated through a bootstrap resampling process showed
336 reductions in AUC from 0.864 to 0.824 for the ADC-radiomic model (Dissimilarity and
337 Energy), from 0.808 to 0.716 for the T2-W radiomic model (Dissimilarity,
338 InverseVariance and ClusterProminence) and from 0.794 to 0.718 for clinico-
339 pathological model (T2-W volume, Depth of Invasion and LVSI). The combined
340 radiomic and clinico-pathological models were corrected from 0.916 to 0.84 (ADC-
341 radiomic and clinico-pathological features) and from 0.906 to 0.822 (T2-W-radiomic
342 and clinico-pathological features).

343 **Discussion**

344 Our data has identified the radiomic features from ADC maps and T2-W images that
345 differ between high- and low-volume cervical tumors and shown that these features
346 individually and in combination are useful for predicting recurrence in low-volume
347 tumors. Patients in the high- and low--volume tumor groups were well matched by
348 age, and although the low-volume tumors were by definition lower stage, there were
349 more adenocarcinomas and LVSI in this group, both of which adversely affect
350 outcome. Radiomic differences between high and low-volume tumors were largely
351 similar for both the ADC and T2-W data although regression models identified
352 different combinations of features as being contributory to prediction of recurrence in
353 each case. Moreover, although radiomic features differed between tumors with and
354 without LVSI, they did not differ between other histological parameters of poor
355 prognosis (type, grade, Depth of Invasion, LN metastasis), indicating that they are
356 likely to be independent.

357 This data highlights the potential of texture feature analysis for predicting recurrence
358 with potential to influence the surgical management of patients with early stage, low-
359 volume cervical cancer. It means that surgical management can be altered, or
360 appropriate patient counselling provided at the outset because the use of adjuvant
361 therapy can be anticipated. The utility of such information would be particularly
362 valuable in a young patient population seeking to retain fertility and minimize
363 therapy. For instance, to avoid the toxicity of lymphadenectomy followed by adjuvant
364 chemoradiation, patients with “good” radiomic features may elect to have sentinel
365 node biopsy prior to curative treatment (surgery or chemoradiation). Additionally,
366 patients could be counselled as to the need for adjuvant therapy at the outset. In
367 larger tumors, where volume is a strong predictive factor of recurrence [31] and

368 survival [32] , the utility of additional radiomic analyses in altering management
369 remains to be established.

370 The greater tendency to decreased Dissimilarity in larger tumors, indicates that grey
371 levels in adjacent pixels were similar in larger tumors. Energy, which is a measure of
372 textural uniformity, and is highest when grey level distribution has either a constant
373 or a periodic form, also was higher in larger tumors. A previous prospective study
374 has confirmed the reproducibility of these features and their lack of dependence on
375 regional ROI selection within the tumor [33], nevertheless we used whole tumor
376 analysis in our study. A study by Hao et al has shown that radiomic analysis of the
377 tumor periphery is informative in differentiating those likely to recur from those that
378 do not [34], but the tumor volume in their cohort was high and patients were treated
379 with chemoradiation. Our data interrogates the differences in features between high-
380 vs. low-volume tumors across the entire tumor volume and uses these features to
381 recognize low- volume tumors with potentially poor prognosis. It confirms for the first
382 time using radiomic analysis, that as cervical tumors grow, they tend to become
383 texturally less dissimilar and more homogenous. This may well reflect the transition
384 from a morphology where tumor elements are interspersed with normal cervical
385 glandular elements and stroma in smaller tumors to more homogenous sheets of
386 malignant cells as tumors increase in size and de-differentiate. The T2W-radiomic
387 features, however, were less good than the ADC-radiomic features for predicting
388 recurrence. They did not offer significant improvements for prediction of recurrence
389 when combined with clinico-pathological features as the model over-fitted the data.
390 T2-W data also was affected by signal-intensity variations across the image,
391 particularly in the presence of an endovaginal coil, which was not an issue with the
392 quantified ADC from diffusion-weighted images.

393 Other retrospective studies have reported radiomic features derived from MRI and
394 ¹⁸F-DG-positron emission tomography (PET) scans of locally advanced cervical
395 cancer treated with chemoradiotherapy. Radiomics features such as entropy from
396 ADC maps and grey level non-uniformity from PET, respectively, have been shown
397 to be independent predictors of recurrence and loco-regional control in these larger
398 volume tumors with significantly higher prognostic power than usual clinical
399 parameters [35]. This supports our findings where these features are shown to differ
400 between high- and low-volume tumors and to be predictive of recurrence in the low-
401 volume tumor group.

402 A strength of this study was the derivation of the data using an endovaginal receiver
403 coil, particularly in small volume tumors where it was possible to obtain a minimum of
404 100 voxels. This provided a substantial boost in SNR [24] and was invaluable for the
405 assessment of the ADC data where external array imaging in the low-volume tumors
406 would have limited the voxel numbers and precluded meaningful ADC feature
407 analysis.

408 The application of adjuvant therapy as a confounding factor represented an analysis
409 dilemma: removal of patients with low-volume tumours on MRI who went on to
410 receive adjuvant chemotherapy would have biased the sample and made it
411 unrepresentative of the final application. On the other hand, retaining these patients
412 in the analysis, potentially weakened the model because patients with MRI radiomics
413 features indicative of a recurrence after surgery will have that recurrence prevented
414 by the adjuvant treatment. Our solution here was to perform both sets of analyses.
415 As predicted, when the patients who received adjuvant therapy were removed, the
416 AUC of the model increased, but at the cost of a smaller sample size.

417 Like many current studies in tumor radiomics, our work has several limitations. First
418 it is a single site study with a relatively small sample size, albeit from a quaternary
419 referral gynaecological oncology centre which sees and treats a high volume of
420 patients. Second, the recurrence rate was low (~10%) but is in keeping with
421 expectations in this early stage, potentially curable disease. Even with a larger
422 sample size, it would not have been possible to avoid such an imbalance between
423 the recurrence and no-recurrence classes. Taken together, these factors lead to a
424 model based on a small number of recurrences and the consequent risk of overfitting
425 from the combined model, with a possibly over-optimistic value for the combined-
426 model AUC. However, we show that for *single-feature* models *any one* of the ADC
427 radiomic features Dissimilarity, Energy, InverseVariance, ClusterProminence,
428 Autocorrelation or ADC volume performed better than the highest-scoring “clinico-
429 pathological” features (T2-W volume and LVSI). Furthermore, when considering
430 models based on just *two* features, the radiomic model (ADC Dissimilarity and
431 Energy, AUC=0.864) compared well with the clinical model (T2-W volume and Depth
432 of invasion, AUC=0.766). Third, patients were often diagnosed following a LLETZ
433 biopsy which may remove a significant volume of disease, thus affecting the
434 assessment at their staging MRI and confounding our results; this was the case in 1
435 patient in our study group. Nevertheless, in a clinical setting a LLETZ or cone biopsy
436 is performed as part of the normal clinical pathway prior to MRI and imaging prior to
437 a diagnostic LLETZ or cone biopsy is unlikely, making our results more applicable in
438 a clinical workflow. In future, when determining the utility of radiomic features
439 combined with other clinical and histologic assessments, use of MRI plus LLETZ
440 volume is desirable. Finally, the current poor availability of endovaginal MRI limits
441 radiomic assessments of low-volume tumors more widely. However, if further

442 accumulation of cases confirms the predictive power of this model and that high SNR
443 enables its implementation, this will provide a justification for more widespread use
444 of this MRI technique at specialist centres offering trachelectomy. Alternatively,
445 improvements of SNR in non-endovaginal MRI may be required.

446 In conclusion, in patients with low-volume tumors, ADC-radiomic texture analysis is
447 potentially a useful predictor of tumor recurrence. This can substantially impact the
448 treatment planning and counselling of patients with low-volume tumors seeking
449 fertility preservation.

450

451

452

453

454

455 **Conflict of interest/disclosure statement**

456 "The authors declare no potential conflicts of interest."

457

458 **Author Contributions**

459 **Ben Wormald:** Conceptualization, Methodology, Data curation, Analysis, Writing-

460 Original draft preparation. **Simon Doran:** Methodology, Data curation, Analysis

461 Supervision. **Thomas Ind: Data Curation, Patient Management. James**

462 **Petts:** Software, Analysis. **James D'Arcy:** Software, Analysis. **Nandita deSouza:**

463 Conceptualization, Writing-Reviewing and Editing, Supervision.

464

465 **REFERENCES**

466 1 Shepherd JH, Spencer C, Herod J, Ind TE (2006) Radical vaginal trachelectomy as a fertility-
467 sparing procedure in women with early-stage cervical cancer-cumulative pregnancy rate in a
468 series of 123 women. *Bjog* 113:719-724

469 2 Bentivegna E, Gouy S, Maulard A, Chargari C, Leary A, Morice P (2016) Oncological outcomes
470 after fertility-sparing surgery for cervical cancer: a systematic review. *Lancet Oncol* 17:e240-
471 e253

472 3 Laios A, Kasius J, Tranoulis A, Gryparis A, Ind T (2018) Obstetric Outcomes in Women With
473 Early Bulky Cervical Cancer Downstaged by Neoadjuvant Chemotherapy to Allow for
474 Fertility-Sparing Surgery: A Meta-analysis and Metaregression

475 4 Naik R, Cross P, Nayar A et al (2007) Conservative surgical management of small-volume
476 stage IB1 cervical cancer. *Bjog* 114:958-963

477 5 Alfsen GC, Kristensen GB, Skovlund E, Pettersen EO, Abeler VM (2001) Histologic subtype has
478 minor importance for overall survival in patients with adenocarcinoma of the uterine cervix.
479 *Cancer* 92:2471-2483

480 6 Horn L-C, Bilek K, Fischer U, Einenkel J, Hentschel B (2014) A cut-off value of 2cm in tumor
481 size is of prognostic value in surgically treated FIGO stage IB cervical cancer. *Gynecologic*
482 *Oncology* 134:42-46

483 7 Halle MK, Ojesina AI, Engerud H et al (2017) Clinicopathologic and molecular markers in
484 cervical carcinoma: a prospective cohort study. *Am J Obstet Gynecol* 217:432.e431-432.e417

485 8 Burke TW, Hoskins WJ, Heller PB, Bibro MC, Weiser EB, Park RC (1987) Prognostic factors
486 associated with radical hysterectomy failure. *Gynecol Oncol* 26:153-159

487 9 Kato T, Takashima A, Kasamatsu T et al (2015) Clinical tumor diameter and prognosis of
488 patients with FIGO stage IB1 cervical cancer (JCOG0806-A). *Gynecologic Oncology* 137:34-39

489 10 Samlal RA, van der Velden J, Ten Kate FJ, Schilthuis MS, Hart AA, Lammes FB (1997) Surgical
490 pathologic factors that predict recurrence in stage IB and IIA cervical carcinoma patients
491 with negative pelvic lymph nodes. *Cancer* 80:1234-1240

492 11 Cibula D, Pötter R, Planchamp F et al (2018) The European Society of Gynaecological
493 Oncology/European Society for Radiotherapy and Oncology/European Society of Pathology
494 guidelines for the management of patients with cervical cancer. *Radiotherapy and Oncology*
495 127:404-416

496 12 Roh HJ, Kim KB, Lee JH, Kim HJ, Kwon YS, Lee SH (2018) Early Cervical Cancer: Predictive
497 Relevance of Preoperative 3-Tesla Multiparametric Magnetic Resonance Imaging. *Int J Surg*
498 *Oncol* 2018:9120753

499 13 Guan Y, Shi H, Chen Y et al (2016) Whole-Lesion Histogram Analysis of Apparent Diffusion
500 Coefficient for the Assessment of Cervical Cancer. *J Comput Assist Tomogr* 40:212-217

501 14 Downey K, Riches SF, Morgan VA et al (2013) Relationship between imaging biomarkers of
502 stage I cervical cancer and poor-prognosis histologic features: quantitative histogram
503 analysis of diffusion-weighted MR images. *AJR Am J Roentgenol* 200:314-320

504 15 Winfield JM, Orton MR, Collins DJ et al (2017) Separation of type and grade in cervical
505 tumours using non-mono-exponential models of diffusion-weighted MRI. *Eur Radiol* 27:627-
506 636

507 16 Guan Y, Li W, Jiang Z et al (2017) Value of whole-lesion apparent diffusion coefficient (ADC)
508 first-order statistics and texture features in clinical staging of cervical cancers. *Clin Radiol*
509 72:951-958

510 17 Woo S, Kim SY, Cho JY, Kim SH (2017) Apparent diffusion coefficient for prediction of
511 parametrial invasion in cervical cancer: a critical evaluation based on stratification to a Likert
512 scale using T2-weighted imaging. *Radiol Med*. 10.1007/s11547-017-0823-x

513 18 Yang W, Qiang JW, Tian HP, Chen B, Wang AJ, Zhao JG (2017) Minimum apparent diffusion
514 coefficient for predicting lymphovascular invasion in invasive cervical cancer. *J Magn Reson*
515 *Imaging* 45:1771-1779

516 19 Meng J, Zhu L, Zhu L et al (2016) Apparent diffusion coefficient histogram shape analysis for
517 monitoring early response in patients with advanced cervical cancers undergoing concurrent
518 chemo-radiotherapy. *Radiat Oncol* 11:141

519 20 Downey K, Jafar M, Attygalle AD et al (2013) Influencing surgical management in patients
520 with carcinoma of the cervix using a T2- and ZOOM-diffusion-weighted endovaginal MRI
521 technique. *Br J Cancer* 109:615-622

522 21 Payne GS, Schmidt M, Morgan VA et al (2010) Evaluation of magnetic resonance diffusion
523 and spectroscopy measurements as predictive biomarkers in stage 1 cervical cancer.
524 *Gynecol Oncol* 116:246-252

525 22 Hou Z, Li S, Ren W, Liu J, Yan J, Wan S (2018) Radiomic analysis in T2W and SPAIR T2W MRI:
526 predict treatment response to chemoradiotherapy in esophageal squamous cell carcinoma. *J*
527 *Thorac Dis* 10:2256-2267

528 23 Wang Q, Li Q, Mi R et al (2019) Radiomics Nomogram Building From Multiparametric MRI to
529 Predict Grade in Patients With Glioma: A Cohort Study. *J Magn Reson Imaging* 49:825-833

530 24 Gilderdale DJ, deSouza NM, Coutts GA et al (1999) Design and use of internal receiver coils
531 for magnetic resonance imaging. *Br J Radiol* 72:1141-1151

532 25 Pecorelli S, Zigliani L, Odicino F (2009) Revised FIGO staging for carcinoma of the cervix.
533 *International Journal of Gynecology & Obstetrics* 105:107-108

534 26 Marcus DS, Olsen TR, Ramaratnam M, Buckner RL (2007) The Extensible Neuroimaging
535 Archive Toolkit: an informatics platform for managing, exploring, and sharing neuroimaging
536 data. *Neuroinformatics* 5:11-34

537 27 Doran SJ, d'Arcy J, Collins DJ et al (2012) Informatics in radiology: development of a research
538 PACS for analysis of functional imaging data in clinical research and clinical trials.
539 *Radiographics* 32:2135-2150

540 28 Blackledge MD, Collins DJ, Koh DM, Leach MO (2016) Rapid development of image analysis
541 research tools: Bridging the gap between researcher and clinician with pyOsiriX. *Comput Biol*
542 *Med* 69:203-212

543 29 Wibmer A, Hricak H, Gondo T et al (2015) Haralick texture analysis of prostate MRI: utility for
544 differentiating non-cancerous prostate from prostate cancer and differentiating prostate
545 cancers with different Gleason scores. *Eur Radiol* 25:2840-2850

546 30 Haralick RM, Shanmugam K, Dinstein I (1973) Textural Features for Image Classification. *IEEE*
547 *Transactions on Systems, Man, and Cybernetics* SMC-3:610-621

548 31 Sethi TK, Bhalla NK, Jena AN, Rawat S, Oberoi R (2005) Magnetic resonance imaging in
549 carcinoma cervix--does it have a prognostic relevance. *J Cancer Res Ther* 1:103-107

550 32 Soutter WP, Hanoch J, D'Arcy T, Dina R, McIndoe GA, DeSouza NM (2004) Pretreatment
551 tumour volume measurement on high-resolution magnetic resonance imaging as a predictor
552 of survival in cervical cancer. *Bjog* 111:741-747

553 33 Liu Y, Zhang Y, Cheng R et al (2018) Radiomics analysis of apparent diffusion coefficient in
554 cervical cancer: A preliminary study on histological grade evaluation. *J Magn Reson Imaging*.
555 10.1002/jmri.26192

556 34 Hao H, Zhou Z, Li S et al (2018) Shell feature: a new radiomics descriptor for predicting
557 distant failure after radiotherapy in non-small cell lung cancer and cervix cancer. *Physics in*
558 *Medicine & Biology* 63:095007

559 35 Lucia F, Visvikis D, Desseroit MC et al (2018) Prediction of outcome using pretreatment
560 (18)F-FDG PET/CT and MRI radiomics in locally advanced cervical cancer treated with
561 chemoradiotherapy. *Eur J Nucl Med Mol Imaging* 45:768-786

562

563

564 **TABLES:**

565 **Table 1:** Patient characteristics for all tumors and for low- and high-volume tumor
566 sub-groups (** 1 treated with chemoradiotherapy*)

567

568 **Table 2:** Texture features derived from ADC maps and T2-W images showing
569 differences between low- and high- volume tumors

570

571 **Table 3:** Texture features derived from ADC maps and T2-W images in 68 low-
572 volume tumors for prediction of recurrence

573

574 **Table 4:** Regression models in prediction of recurrence with bootstrap corrected
575 AUC and Chi-Square test of model differences. The reduction in AIC when ADC-
576 radiomic and clinico-pathological features are combined compared to clinico-
577 pathological features alone is indicative of the improvement of the combined model.

578

579

580 **FIGURE LEGENDS**

581 **Figure 1:** T2-W (a) and ADC map (b) in a 33- year old patient with a 0.8 cm³ volume
582 tumor that had high dissimilarity (0.808). Regions-of-interest delineate the tumor.
583 The intermediate signal-intensity tumor on the T2-W imaging (arrow) is restricted in
584 diffusion on the ADC maps (arrow). Tumor was confined to the cervix, and the
585 patient remains disease-free following trachelectomy. T2-W (c) and ADC map (d) in
586 a 26 year old patient with a 0.9 cm³ volume tumor that had low dissimilarity (0.489).
587 The intermediate signal-intensity tumor on the T2-W imaging (c) is restricted in
588 diffusion on the ADC maps (d). Regions-of-interest delineate the tumor. Tumor was
589 confined to the cervix, but despite negative nodes on surgical histology, the patient
590 recurred centrally after 9 months.

591

592 **Figure 2:** Receiver Operating Curves showing sensitivity and specificity for
593 prediction of recurrence by texture and clinic-pathological features (a) in 68 patients
594 with low-volume tumors where use of adjuvant therapy is included in the model; (b)
595 in 54 patients who did not receive adjuvant therapy; and (c) in all 68 patients using
596 features identified in both a and b (Dissimilarity, Energy for ADC-radiomics;
597 Dissimilarity, ClusterProminence, InverseVariance for T2-W-radiomics; and Volume,
598 Depth of Invasion, LymphoVascular Space Invasion for clinico-pathological
599 features). In a, no combination of T2-W features was significantly superior to
600 individual features. In b, of the clinico-pathological features, LVSI alone was
601 predictive of recurrence, In c, the optimal prediction of recurrence is shown by a
602 combination of ADC-radiomic an clinico-pathological features.

603

Table 1: Patient characteristics for all tumors and for low- and high-volume tumor subgroups (* 1 treated with chemoradiotherapy)

	All tumors	High volume >4.19cm ³	Low volume <4.19cm ³
Age, mean (range)	38.4 (65.0)	43.0 (64.0)	35.6 (38.0)
BMI, mean (range)	25.7 (36.3)	26.2 (36.3)	25.4 (32.9)
FIGO stage, n			
1	74	69	5
2	51	10	41
Histological subtype, % patients (n)			
Squamous	61.6 (77)	78.3 (36)	51.9 (41)
Adenocarcinoma	38.4 (48)	21.7 (10)	48.1 (38)
Grade % patients (n)			
1 or 2	55.2 (69)	52.2 (24)	57.0 (45)
3	43.2 (54)	43.5 (20)	43.0 (34)
Unknown	1.6 (2)	4.3 (2)	0
LVSI, % patients (n)			
Positive	27.2 (34)	15.2 (7)	34.2 (27)
Negative	65.6 (82)	67.4 (31)	64.6 (51)
Unknown	7.2 (9)	17.4 (8)	1.2 (1)
Depth of Invasion, mean (range)	7.1 (20.4)	6.0 (19.0)	7.4 (20.4)
Parametrial invasion % patients (n)			
Positive	32.8 (41)	76.1 (35)	7.6 (6)
Negative	67.2 (84)	23.9 (11)	92.4 (73)
Lymph node metastasis, % patients (n)			
Positive	31.2 (39)	58.7 (27)	15.2 (12)
Negative	68.8 (86)	41.3 (19)	84.8 (67)
Treatment, % patients (n)			
Surgery	61.6 (77)	15.2 (7)	88.6 (70)
Chemoradiation	38.4 (48)	84.8 (39)	11.4 (9)
Surgery, % patients (n)			
Cold Knife Cone CKC	0	0	0
Trachelectomy	48.1 (37)	14.3 (1)	51.4 (36)
Hysterectomy	51.9 (40)	85.7 (6)	48.6 (34)
Adjuvant treatment after surgery % patients (n)			
Yes	23.4 (18)	28.6 (2)	22.9 (16)
Recurrence, % patients (n)			
Yes	16.0 (20)	26.1 (12)	10.1 (8)*
No	78.4 (98)	65.2 (30)	86.1 (68)
Unknown	5.6 (7)	8.7 (4)	3.8 (3)

Table 2: Texture features derived from ADC maps and T2-W images showing differences between low- and high- volume tumors

		Median low volume N=79	IQR low volume N=79	Median high volume N=46	IQR high volume N=46	Adjusted p-value
Dissimilarity	ADC	0.64	0.28	0.35	0.17	1.22E-11
	T2W	0.49	0.32	0.25	0.12	4.31E-14
Energy	ADC	0.15	0.11	0.30	0.21	3.76E-09
	T2W	0.20	0.13	0.34	0.2	7.55E-10
InverseVariance	ADC	0.41	0.08	0.29	0.13	2.84E-11
	T2W	0.38	0.12	0.23	0.10	9.61E-13
ClusterProminence	ADC	29.33	40.77	10.52	10.11	5.95E-08
	T2W	22.66	24.14	8.03	6.50	1.49E-09
ClusterShade	ADC	2.82	3.62	1.26	1.42	3.84E-03
	T2W	2.29	2.28	1.18	1.30	0.02
Autocorrelation	ADC	11.41	5.68	9.13	4.64	0.02
	T2W	11.65	8.69	6.08	3.64	8.22E-09
InformationalMeasure Correlation2	ADC	0.63	0.21	0.54	0.07	0.08
	T2W	0.67	0.16	0.68	0.22	1
Correlation	ADC	0.44	0.18	0.47	0.07	0.89
	T2W	0.55	0.23	0.62	0.26	0.03

Table 3: Texture features derived from ADC maps and T2-W images in 68 low-volume tumors for prediction of recurrence

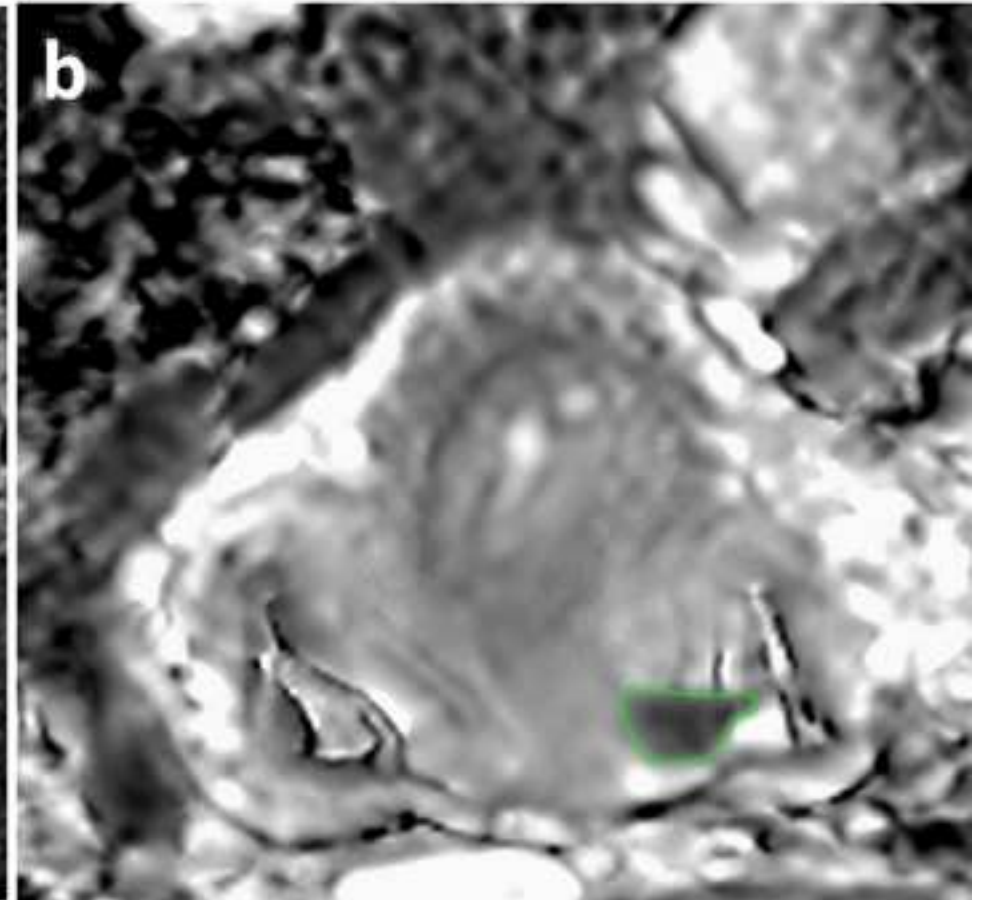
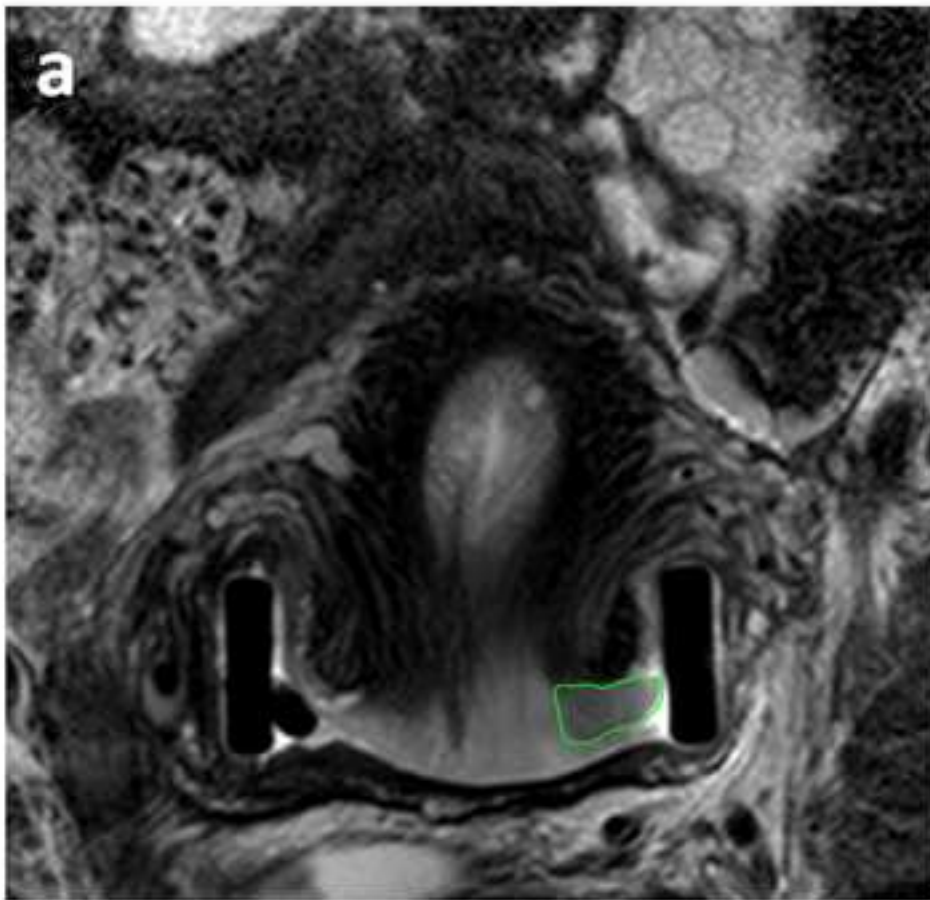
Texture feature	From	AUC (CI)	Threshold	Sensitivity	Specificity
Dissimilarity	ADC map	0.775 (0.646-0.904)	0.635	100	61
	T2-W image	0.609 (0.334-0.883)	0.318	43	89
Energy	ADC map	0.635 (0.432-0.838)	0.178	71	61
	T2-W image	0.604 (0.373-0.835)	0.235	71	67
Cluster prominence	ADC map	0.646 (0.425-0.868)	53.789	100	33
	T2-W image	0.607 (0.364-0.849)	12.113	43	85
Inverse variance	ADC map	0.674 (0.496-0.853)	0.443	100	38
	T2-W image	0.665 (0.444-0.886)	0.349	71	66
Auto-correlation	ADC map	0.665 (0.497-0.833)	11.978	100	41
	T2-W image	0.628 (0.463-0.793)	8.921	100	38
Correlation	ADC map	-	-	-	-
	T2-W image	0.536 (0.326-0.746)	0.524	71	57
ClusterShade	ADC map	0.508 (0.292-0.724)	5.75	100	23
	T2-W image	0.511 (0.274-0.747)	3.474	86	26
InformationMeasureCorrelation2	ADC map	-	-	-	-
	T2-W image	-	-	-	-
Volume	ADC map	0.672 (0.426-0.919)	1292.136	71	64
	T2-W image	0.691 (0.448-0.936)	1248.191	71	64

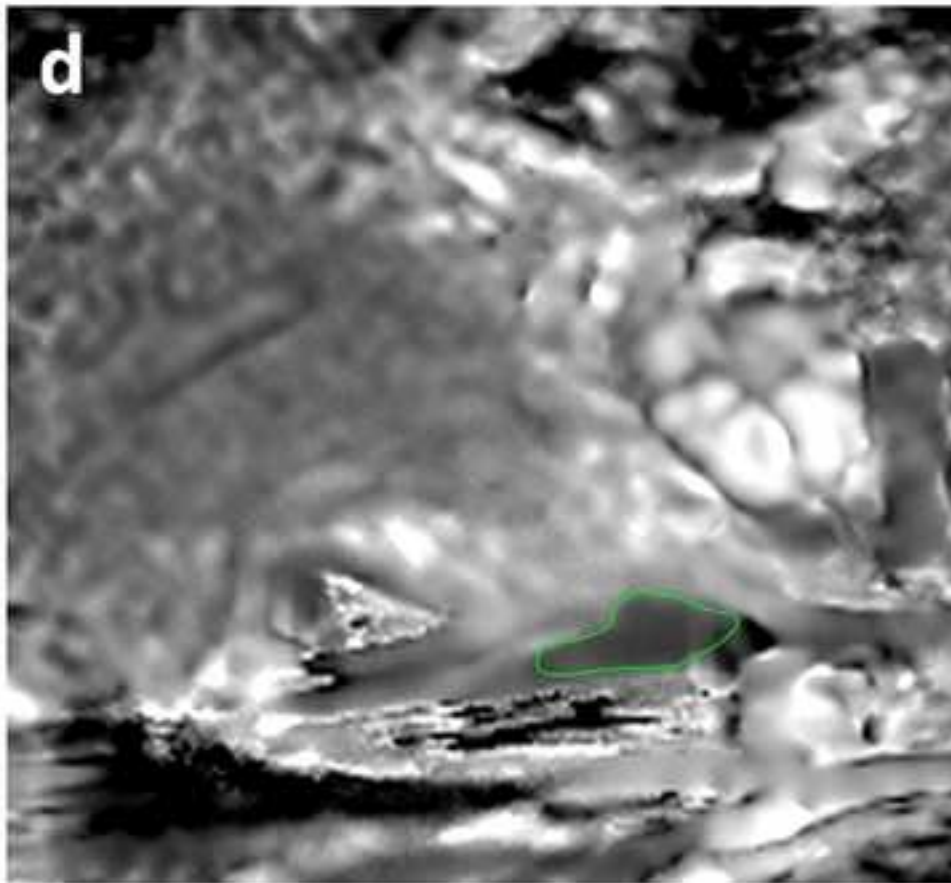
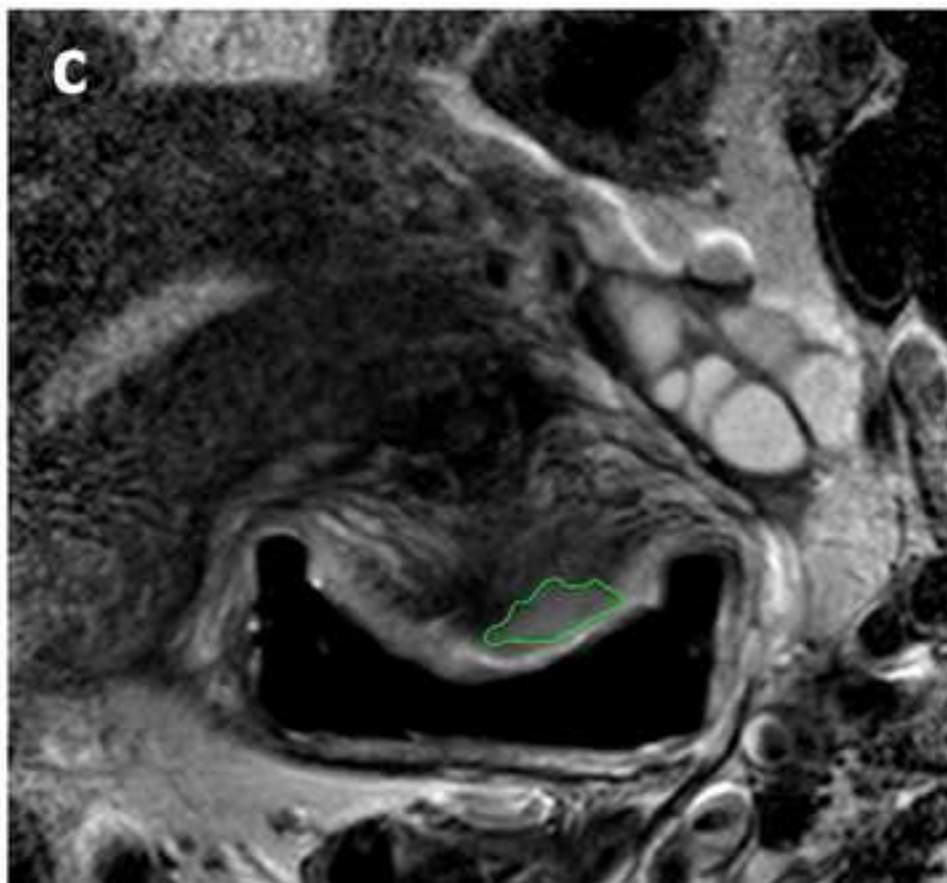
Table 4: Regression models in prediction of recurrence with bootstrap corrected AUC and Chi-Square test of model differences. The reduction in AIC when ADC-radiomic and clinico-pathological features are combined compared to clinico-pathological features alone is indicative of the improvement of the combined model.

	AUC	CI	Corrected AUC	AIC	Resid. Df	Resid. Dev	Df	Deviance	p Value*
Clinico-pathological	0.794	0.617-0.971	0.708	45.684	64	37.684	-	-	-
ADC-Radiomic	0.864	0.772-0.956	0.824	41.044	65	-	-	-	-
T2W-Radiomic	0.808	0.690-0.926	0.716	49.193	65	-	-	-	-
ADC-Radiomic +Clinico-pathological	0.916	0.837-0.994	0.840	39.638	63	27.638	2	10.046	0.006
T2W-Radiomic +Clinico-pathological	0.906	0.822-0.991	0.822	45.128	61	31.128	3	6.556	0.086

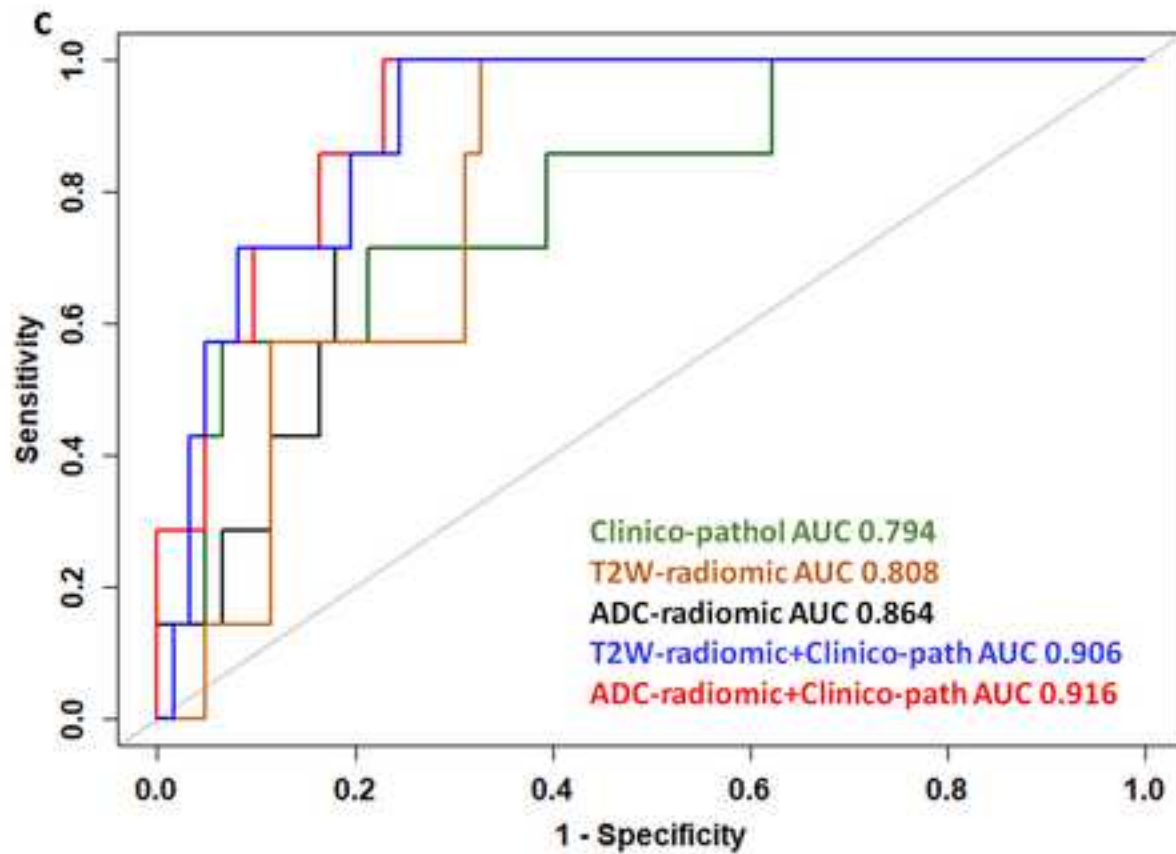
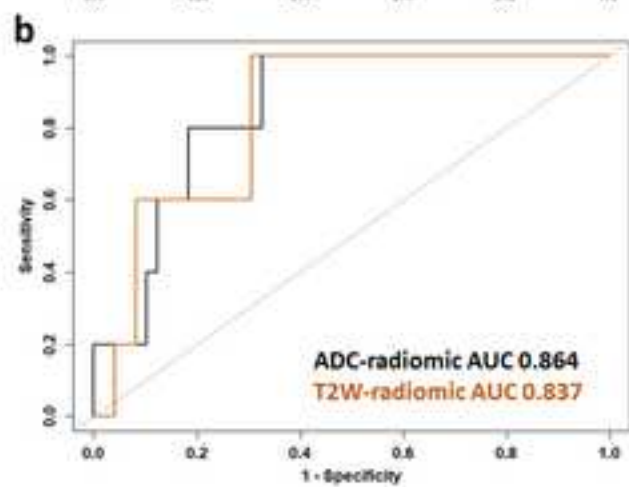
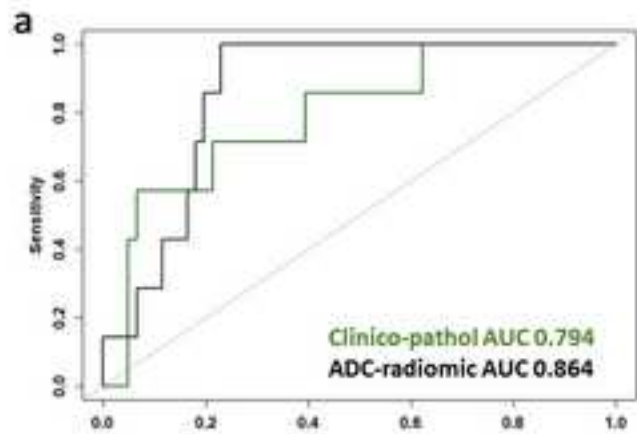
*p- value of nested model compared to clinico-pathological model.

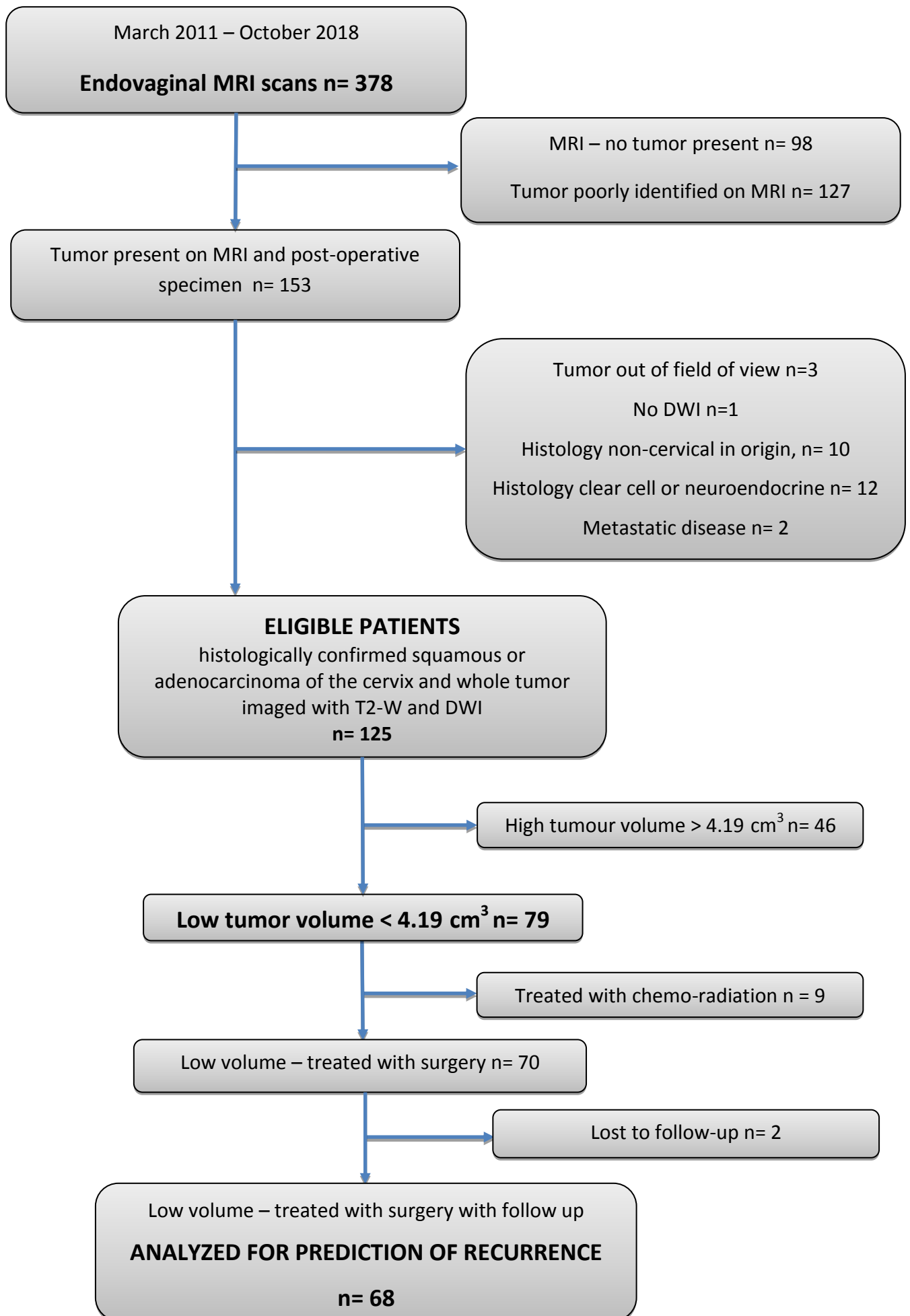
5. Figure 1a_b
[Click here to download high resolution image](#)





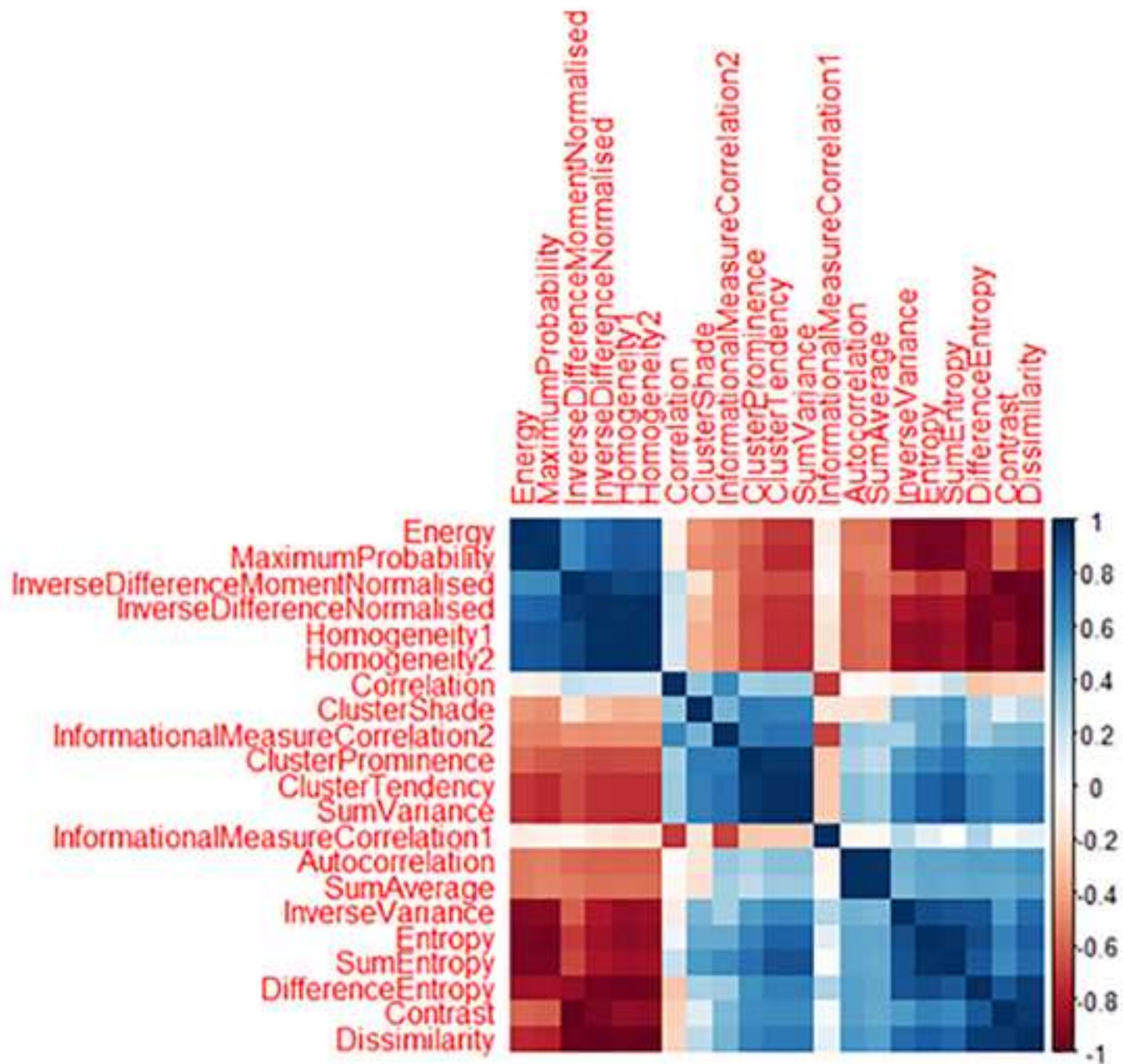
5. Figure 2
[Click here to download high resolution image](#)





6. Figure S2

[Click here to download high resolution image](#)



Highlights

1. Texture features differed significantly between high- compared to low-volume cervical tumors ($p < 0.02$).
2. In low-volume tumors, predicting recurrence from ADC-radiomics was superior to T2-W-radiomics or clinico-pathologic features.
3. Combining ADC-radiomic and clinico-pathologic features together improved recurrence prediction further.

Statement of Translational Relevance:

This data indicates that in small volume cervical cancers suitable for trachelectomy, a combination of radiomic features derived from ADC maps on MRI and clinico-pathological factors best predicts likelihood of recurrence. These patients are currently selected for adjuvant therapy based on clinico-pathological features post-trachelectomy. Although selection of patients for adjuvant therapy based on imaging radiomic features as predictors of recurrence requires further validation in a test set, the robustness of our data as indicated by bootstrap re-sampling technique, warrants close follow-up of individuals with tumors exhibiting poor radiomic features. We suggest that in patients with tumors $< 4 \text{ cm}^3$ treated surgically, where ADC-radiomics show that Dissimilarity is high and Energy low, introduction of more frequent vault smears and imaging in the first 3 years post-operatively would help identify recurrences early.

CRedit author statement

Ben Wormald: Conceptualization, Methodology, Data curation, Analysis, Writing-Original draft preparation. **Simon Doran:** Methodology, Data curation, Analysis Supervision. **Thomas Ind:** Data Curation, Patient Management. **James Petts:** Software, Analysis. **James D'Arcy:** Software, Analysis. **Nandita deSouza:** Conceptualization, Writing-Reviewing and Editing, Supervision.